Available online at www.sciencedirect.com
SCIENCE DIRECT®
Journal of Sound and Vibration 291 (2006) 1004–1028
JOURNAL OF SOUND AND VIBRATION
www.elsevier.com/locate/jsvi

Analysis and design of passive band-stop filter-type vibration isolators for low-frequency applications

C. Yilmaz*, N. Kikuchi

Department of Mechanical Engineering, University of Michigan, Ann Arbor, MI 48109, USA

Received 17 March 2005; received in revised form 27 June 2005; accepted 7 July 2005
Available online 24 August 2005

Abstract

The aim of this paper is to design a stiff and lightweight passive vibration isolator that has wide stop-band at low frequencies. First of all, bandwidths of single-degree-of-freedom (sdof) dynamic vibration absorbers and lever-type anti-resonant vibration isolators are formulated in a general framework. Then, by making use of these formulations, a 2dof vibration isolator is synthesized to obtain large bandwidth at low frequencies. It has been shown that inertial coupling was beneficial in obtaining a stiff and lightweight design. More importantly, asymmetry in the inertial forcing terms generated by the levered masses yielded a vibration isolator that has two anti-resonance frequencies in its stop-band. Finally, bandwidth improvement over the previously analyzed isolators is demonstrated via numerical examples.

1. Introduction

This paper is about undamped band-stop filter-type vibration isolators used in the case of harmonic base excitation. The term ''band-stop filter'' is used to emphasize that all the isolator designs in this paper achieve isolation in some frequency intervals denoted by stop-bands. The focus is on stiff isolator designs for low-frequency applications. More precisely, the stop-bands of the designs considered in this paper are at frequencies smaller than the natural frequencies of equivalently stiff isolation systems in which the isolators are massless springs. There are basically

*Corresponding author. Tel.: +1 734 936 2926; fax: +1 734 647 3170.
E-mail addresses: cyilmaz@umich.edu (C. Yilmaz), kikuchi@umich.edu (N. Kikuchi).

0022-460X/$ - see front matter © 2005 Elsevier Ltd. All rights reserved.
doi:10.1016/j.jsv.2005.07.019

Nomenclature

AMD	auxiliary mass damper
BW	normalized bandwidth of a stop-band
BW_a	normalized bandwidth of a single dynamic vibration absorber equipped load
BW_I	normalized bandwidth of a Type I anti-resonant vibration isolator
BW_{II}	normalized bandwidth of a Type II anti-resonant vibration isolator
DAVI	dynamic anti-resonant vibration isolator
DVA	dynamic vibration absorber
F	forcing vector
HEM	hydraulic engine mount
k	overall stiffness of an isolation system from the base to the load
k_a	absorber spring stiffness in the case of a dynamic vibration absorber equipped load
k_i	stiffness of the ith spring in the 2-degree-of-freedom optimum band-stop filter-type isolator
K	stiffness matrix
l_1	length of the lever in the case of single-degree-of-freedom lever-type anti-resonant vibration isolators
l_2	distance between two pivot points in the case of single-degree-of-freedom lever-type anti-resonant vibration isolators
m	load mass
m_a	absorber mass in the case of a dynamic vibration absorber equipped load
m_i	ith isolator mass in the 2-degree-of-freedom optimum band-stop filter-type isolators
m_{is}	total mass of the isolator
M	mass matrix
mdof	multi-degree-of-freedom
N	ratio of natural frequency of the primary structure to the center frequency of the stop-band where the primary structure is modeled as a load with mass m supported on a base by a spring with stiffness k without any additional absorbers or isolators
r	normalized excitation frequency
R_{bw}	ratio of normalized bandwidth of a 2-degree-of-freedom optimum band-stop filter-type isolator to the bandwidth of an equivalent Type II anti-resonant vibration isolator
sdof	single-degree-of-freedom
$T(\omega)$	transmissibility
T_0	maximum allowable transmissibility in the stop-band
x	displacement of load
x_i	displacement of the upper end of the ith isolator spring in the 2-degree-of-freedom optimum band-stop filter-type isolators
X	displacement amplitude of load
X	displacement vector
y	displacement of base
Y	displacement amplitude of base
z	displacement of the absorber mass in dynamic vibration absorber equipped loads or displacement of the isolator mass in the case of single-degree-of-freedom lever-type anti-resonant vibration isolators
α	lever ratio in single-degree-of-freedom lever-type anti-resonant vibration isolators
α_i	lever ratio of the ith isolator stage in the 2-degree-of-freedom optimum band-stop filter-type isolators
μ	ratio of isolator or absorber mass to load mass
ω	excitation frequency
ω_a	anti-resonance frequency in the case of a dynamic vibration absorber equipped load
ω_c	center frequency of a stop-band
ω_p	resonance frequency (pole) of a system having a single pole
ω_{pi}	ith resonance frequency (pole)
ω_{peak}	local peak frequency in the transmissibility plot of a 2-degree-of-freedom optimum band-stop filter-type isolator
ω_{s}	stop-band frequency of a single-degree-of-freedom mass–spring system

ω_{s1}	lower stop-band frequency	ω_{zi}	ith anti-resonance frequency (zero)
ω_{s2}	higher stop-band frequency	ω_0	natural frequency of a single-degree-of-freedom mass–spring system with mass m and stiffness k
ω_z	anti-resonance frequency (zero) of a system having a single zero		

two different kinds of band-stop filter-type vibration isolators. In the first kind, stop-bands are formed solely by resonance frequencies. In the second kind, stop-bands are formed by anti-resonance frequencies.

Forming stop-bands only by resonance frequencies is a well-established method [1], and can be realized by elastic band-gap structures. These are periodic structures that possess stop-bands due to clever placement of the resonance frequencies. When resonance frequencies are clustered in certain frequency ranges, then there will be very good attenuation in the frequency ranges where no resonance frequency is present. Typically, there are multiple repeated unit cells in these structures. So, there are multiple resonance frequencies prior to the first stop-band, and the stop-band is placed at a quite high frequency relative to the fundamental frequency of the band-gap structure. When a band-gap structure is to be used as a vibration isolator, it should support an object (load) that is to be protected. In that case, the fundamental frequency of the overall system would be even lower than that of the band-gap structure. Although band-gap structures can be promising for various applications (see Refs. [2,3] and the references therein), a band-gap structure cannot be classified as a stiff vibration isolator, unless its mass is much larger than the mass of the object (load) it supports for isolation. So, these systems will not be considered in this paper.

On the other hand, anti-resonance frequencies enable placing stop-bands at very low frequencies without the need of excessive isolator masses. In a linear lumped parameter system, anti-resonance frequencies can be generated by two different methods. The first method is to add a Dynamic Vibration Absorber (DVA). The second method is to generate inertial coupling.

DVAs were introduced by Frahm [4] in the beginning of the 20th century. A single-degree-of-freedom (sdof) DVA basically consists of a mass supported by an undamped spring (similar systems with damping are called as Auxiliary Mass Dampers (AMDs) and used for reducing amplification not for isolation [5]). When a DVA is attached to a primary vibrating structure, it is not attached in the load path. Thus, the stiffness of the system is not changed. By choosing the stiffness and the mass of a sdof DVA accordingly, one can place an anti-resonance (zero) at any frequency, but the DVA also adds another resonance frequency (pole) to the system. The zero forms the stop-band of the system. Since the stop-band is generated by a single anti-resonance frequency, sdof DVAs can mainly be used for tonal applications unless active means of control are applied [6].

As mentioned before, there is a second method to generate anti-resonance frequencies in a system, that is, inertial coupling. Vibration isolators that utilize inertial coupling to generate anti-resonance frequencies were first developed in the 1960s by researchers in the aerospace industry. The development of a new kind of vibration isolator was due to strict requirements on stiffness and mass of the isolators used in the aerospace industry. Flannelly [7] called this new system as

Dynamic Anti-resonant Vibration Isolator (DAVI). DAVI uses a levered mass–spring combination to generate an anti-resonance frequency (zero) in the system. Anti-resonance occurs when the inertial force generated by the levered mass cancels the spring force. This happens at a particular frequency, which depends on the mass of the isolator, the lever ratio and the spring stiffness.

Unlike DVAs, DAVIs are implemented on the load path; therefore the dof of the system is not increased. Furthermore, when a DAVI is introduced to a sdof system, inertial forces generated by the levered mass increases the effective mass of the system. Thus, the resonance frequency decreases and the isolator is capable of operating in a lower-frequency range. For applications in the aerospace industry, please refer to Rita et al. [8], Braun [9,10], Desjardins [11], Desjardins and Hooper [12]. Moreover, Ivovich and Savovich [13] show an application of this system for reduction of low frequency excitations transmitted from machines to their floor supports.

Rivin [14] demonstrates that the rectilinear motion of a primary structure can be transformed into rotary motion by a flywheel and a ball screw, which can also be used to generate the desired inertial forces to generate a zero in the system. The rotational analog of the leverage of Flannelly [7] is the low helix angle of the ball screw.

A couple of years before Flannelly [7], Goodwin [15] also designed an anti-resonant vibration isolator with the same principle. However, he used hydraulic leverage instead of mechanical leverage. Fluid-type systems can provide higher leverage than the mechanical ones. Thus, a small mass of a fluid could generate the desired inertial forces, enabling weight savings on the system. Later, Halwes [16] also designed a fluid-type anti-resonant vibration isolator with the same basic principle. Please refer to Braun [9,10], Smith and Redinger [17], and McGuire [18] for more information.

In the automotive industry, a similar kind of isolator was introduced in the 1980s to replace the rubber engine mounts that do not offer much control on damping and stiffness. Corcoran and Ticks [19], and Flower [20] explain the basic principles of Hydraulic Engine Mounts (HEMs). HEMs having the so-called ''inertia track'' share the same basic principle with the designs of Goodwin [15] and Halwes [16].

Whatever kind of leverage an anti-resonant vibration isolator has, the basic operational principle is the same, and all have a bandwidth limited by a single anti-resonance frequency in their stop-bands. Consequently, active systems were developed in order to increase bandwidth, which in turn decreased the isolators' sensitivity to changes in system parameters due to temperature variation or time, and also increased the tolerance to input frequency variations. Please refer to Smith and Redinger [17], McGuire [18], and Smith et al. [21] for more information on active anti-resonant vibration isolators.

Actually, passive anti-resonant vibration isolators have the potential to be converted into band-stop filter-type vibration isolators that have multiple anti-resonance frequencies within their stop-bands. If they are designed properly, they can have larger bandwidth than the sdof isolator designs especially at low frequencies. This would increase the applicability range of passive isolators. However, to the authors' knowledge, this potential of increasing bandwidth at low frequencies has not been investigated, yet.

In this paper, first of all, bandwidths of DVAs and sdof anti-resonant vibration isolators will be formulated in a general framework. The purpose is to show the limitations and

potentials of these designs particularly in the low-frequency range. Then, a 2dof passive vibration isolator having two anti-resonance frequencies in its stop-band will be designed. The bandwidth improvement over the previously analyzed isolators will be demonstrated via numerical examples.

2. Bandwidth formulations

In the literature, DVAs have been analyzed extensively and lever-type anti-resonant vibration isolators have been analyzed to some extent. However, to the authors' knowledge, there is not much work done in terms of formulating bandwidths of these systems in a general framework.

In this paper, bandwidth formulations for DVA equipped systems and anti-resonant vibration isolators will be based on three non-dimensional numbers, N, μ and T_0. T_0 is the maximum transmissibility that is allowable in the stop-band, μ is the ratio of absorber or isolator mass to load mass, and N is the ratio of natural frequency of the primary structure to the center frequency of the stop-band. The primary structure is modeled as a load supported on a base by a spring without any additional absorbers or isolators. In all the calculations, the springs are assumed to be massless, linear and undamped. The masses and the base are assumed to be rigid. The base excitation motion is harmonic.

The primary structure is a sdof low-pass filter. Hence, given the mass of the load, m, and spring stiffness, k, the primary structure can satisfy a transmissibility requirement, T_0, if the base excitation frequency is larger than the stop-band frequency, ω_s.

$$T_0 = \frac{1}{\omega_s^2/\omega_0^2 - 1}, \quad \text{where } \omega_0 = \sqrt{\frac{k}{m}} \Rightarrow \omega_s = \omega_0\sqrt{1 + \frac{1}{T_0}}. \tag{1}$$

However, in most isolation problems, maximum allowable transmissibility is much less than one, that is, $T_0 \ll 1$. Hence, ω_s is typically large compared to ω_0. Most of the times, there is a minimum stiffness requirement that limits how low can k/m be. So, the stiffness requirement also limits how low can ω_s be.

In this paper, what is meant by low-frequency isolation is that the center frequency of the stop-band is to be placed lower than the natural frequency of the primary structure. Hence, in all the bandwidth formulations N will be greater than one. If N is greater than one, then stiffness is not compromised to satisfy the transmissibility requirement. In other words, if the stop-band is to be placed at a particular frequency, then the stiffness of the system can be made large by choosing N large enough. However, it will be shown that for both DVA equipped systems and lever-type anti-resonant vibration isolators, bandwidth of the stop-band decreases as N gets larger than a certain value. Yet, for low N values, dependence is not straightforward. On the other hand, bandwidth of all these systems decrease as T_0 gets smaller. But, the effect of μ to bandwidth is not again straightforward. To see all these dependences explicitly, bandwidth of DVA equipped systems and anti-resonant vibration isolators will be first formulated based on the three non-dimensional numbers, N, μ and T_0, and then these systems will be compared.

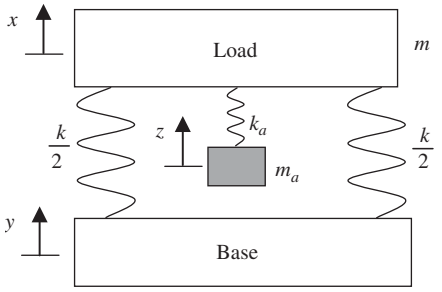

Fig. 1. Base-excited load equipped with a sdof DVA: here, y is the displacement of the base, x is the displacement of the load, z is the displacement of the absorber mass, k is the mount stiffness, m is the mass of the load, k_a is the absorber spring stiffness and m_a is the absorber mass.

2.1. Dynamic vibration absorbers

Let us analyze the system shown in Fig. 1, which is composed of a DVA equipped load that is supported on springs.

Here are the equations of motion for the system in the case of base excitation with zero damping:

$$\begin{bmatrix} m & 0 \\ 0 & m_a \end{bmatrix} \begin{bmatrix} \ddot{x} \\ \ddot{z} \end{bmatrix} + \begin{bmatrix} k + k_a & -k_a \\ -k_a & k_a \end{bmatrix} \begin{bmatrix} x \\ z \end{bmatrix} = \begin{bmatrix} k\,y \\ 0 \end{bmatrix}. \tag{2}$$

Assuming harmonic motion with frequency ω

$$x = X\mathrm{e}^{\mathrm{i}\omega t}, \quad y = Y\mathrm{e}^{\mathrm{i}\omega t}, \quad z = Z\mathrm{e}^{\mathrm{i}\omega t}, \tag{3}$$

the following relationships are obtained:

$$\frac{X}{Y} = \frac{(k_a - m_a\omega^2)k}{(k + k_a - m\omega^2)(k_a - m_a\omega^2) - k_a^2}, \quad \frac{Z}{Y} = \frac{k_a k}{(k + k_a - m\omega^2)(k_a - m_a\omega^2) - k_a^2}. \tag{4}$$

In the literature transmissibility is often defined as the absolute value of the output-to-input displacement amplitude ratio. This definition enables visually appealing transmissibility versus excitation frequency graphs. However, in this paper there will be lots of calculations that involve equating a transmissibility function to a particular value and solving for the frequency that satisfies that equality. To decrease the number of steps in these calculations, the transmissibility function is defined without an absolute value sign. However, for the graphs, absolute value of the transmissibility will be used. So, according to the definition in this paper, $T(\omega)$ is given by the first relationship in Eq. (4). To normalize this equation, let us use the following substitutions:

$$\omega_0 = \sqrt{k/m}, \quad \omega_a = \sqrt{k_a/m_a}, \quad \mu = m_a/m. \tag{5}$$

Then, $T(\omega)$ is obtained as

$$T(\omega) = \frac{(1 - \omega^2/\omega_a^2)}{(1 - \omega^2/\omega_a^2)(1 - \omega^2/\omega_0^2) - (\omega^2/\omega_0^2)\mu}. \tag{6}$$

Let us consider the zero (ω_z) and the poles (ω_{p1}, ω_{p2}) of Eq. (6) in terms of ω^2.

$$\omega_z^2 = \omega_a^2, \tag{7}$$

$$\omega_{p1,2}^2 = \frac{\omega_a^2(\mu+1)+\omega_0^2}{2} \pm \sqrt{\left(\frac{\omega_a^2(\mu-1)+\omega_0^2}{2}\right)^2 + \omega_a^2\mu}. \tag{8}$$

Using Eqs. (7) and (8) one can get the following identity:

$$\omega_{p1,2}^2 - \omega_z^2 = a \pm \sqrt{a^2+b}, \text{ where } a = \frac{\omega_a^2(\mu-1)+\omega_0^2}{2}, \; b = \omega_a^2\mu. \tag{9}$$

Let the smaller pole to be indexed as 1. $\mu>0$, $\omega_a>0$ implies that $b>0$, thus

$$\omega_{p1}^2 - \omega_z^2 = a - \sqrt{a^2+b} < 0, \;\; \omega_{p2}^2 - \omega_z^2 = a + \sqrt{a^2+b} > 0. \tag{10}$$

Therefore,

$$\omega_{p1}^2 < \omega_z^2 < \omega_{p2}^2. \tag{11}$$

Now, let us determine the bandwidth of a DVA equipped system at a given level of transmissibility, T_0, which is a constant. To determine the bandwidth, one should equate the absolute value of Eq. (6) to the given value of T_0 and solve for the two ω^2 values that will yield the two stop-band frequencies (ω_{s1}^2, ω_{s2}^2). Let the smaller stop-band frequency to be indexed as 1, then using Eq. (11), one can get

$$\omega_{p1}^2 < \omega_{s1}^2 < \omega_z^2 < \omega_{s2}^2 < \omega_{p2}^2. \tag{12}$$

In this paper bandwidth, BW, is defined as the normalized bandwidth of a stop-band.

$$BW = (\omega_{s2} - \omega_{s1})/\sqrt{\omega_{s1}\omega_{s2}}. \tag{13}$$

Given T_0, to determine the bandwidth one should solve for ω_{s1}, ω_{s2}. However, to simplify the calculations let us introduce the following relations:

$$\omega_0^2 = N^2\omega_a^2, \;\; \omega_{s1}^2 = l^2\omega_a^2, \;\; \omega_{s2}^2 = u^2\omega_a^2. \tag{14}$$

In low-frequency vibration isolation applications N is greater than one, which implies that the stop-band is placed at a frequency that is lower than the primary system's natural frequency without the absorber. Moreover, Eqs. (7), (12) and (14) imply that u is greater than one and l is less than one. Then, using the above substitutions in Eq. (6) yields u^2 as

$$u^2 = -\frac{(d-e)}{2} + \sqrt{\left(\frac{d-e}{2}\right)^2 + d}, \text{ where } d = N^2\left(\frac{1}{T_0} - 1\right), \;\; e = 1+\mu. \tag{15}$$

Given $N>1$, let us assume that $0<\mu<N^2$ and $T_0 \ll 1$. Then, $d \gg e>1$. Hence, u^2 can be approximated as follows:

$$u^2 = -\frac{(d-e)}{2} + \sqrt{\left(\frac{d-e}{2}\right)^2 + d} = -\frac{(d-e)}{2} + \left(\frac{(d+2-e)}{2}\sqrt{1+\frac{(4e-4)}{(d+2-e)^2}}\right)$$

$$\Rightarrow u^2 \cong -\frac{(d-e)}{2} + \left(\frac{(d+2-e)}{2}\left(1+\frac{(2e-2)}{(d+2-e)^2}\right)\right) = 1+\frac{e-1}{(d+2-e)}. \tag{16}$$

So far, the calculations involved frequency squares. Now, assuming positive frequencies, u can be approximated as follows:

$$u \cong 1+\frac{e-1}{2(d+2-e)} = 1+\frac{\mu}{(2N^2/T_0)-(2N^2-2(1-\mu))}. \tag{17}$$

To find l, one should equate Eq. (6) to $-T_0$. The result can easily be obtained by replacing T_0 with $-T_0$ in Eq. (17) provided that $N>1$, $0<\mu<N^2$ and $T_0 \ll 1$.

$$l \cong 1-\frac{\mu}{(2N^2/T_0)+(2N^2-2(1-\mu))}. \tag{18}$$

$N>1$, $0<\mu<N^2$ and $T_0 \ll 1$. imply that $u \cong 1$ and $l \cong 1$. Thus, Eq. (13) can be used to obtain the approximate value of bandwidth of a DVA equipped system as

$$BW_a = \frac{\omega_{s2}-\omega_{s1}}{\sqrt{\omega_{s1}\omega_{s2}}} = \frac{u-l}{\sqrt{ul}} \cong u-l \cong \frac{T_0\mu}{N^2}. \tag{19}$$

Eq. (19) establishes the dependence of bandwidth to the basic parameters N, μ and T_0. A more exact formulation could be obtained by including higher-order terms in the approximations. However, this has been avoided for the sake of clarity.

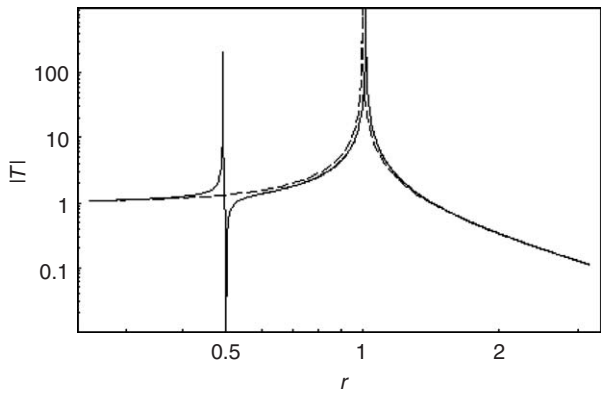

Fig. 2. Transmissibility plots showing the bandwidth of a DVA equipped load for $N=2$, $\mu=0.1$:——, DVA equipped load; – – – –, sdof mass–spring.

Here is an example system with $m = 1$, $k = 1$, $m_a = 0.1$, $k_a = 0.025$. According to these values, the system without an absorber has $\omega_0 = 1$, and the absorber introduces a zero at $\omega_z = 0.5$. Hence, $N = 2$ and $\mu = 0.1$. Fig. 2 shows the transmissibility plots of the DVA equipped load and the sdof mass–spring system without the DVA.

Let us calculate the bandwidth at $T_0 = 0.1$. According to Eq. (19), bandwidth is approximately equal to 0.0025, which is quite a small value. This small bandwidth is barely visible in Fig. 2.

2.2. Lever-type anti-resonant vibration isolators

As mentioned previously, the basic operational principle of the mechanically or hydraulically leveraged anti-resonant vibration isolators are the same. However, for the sake of clarity in the analysis, simple levers will be used to model leverage in anti-resonant vibration isolators.

Depending on the order of the pivot points of the lever with respect to the load and the isolator mass, there are two different types of anti-resonant vibration isolators. Let us call them as Type I and Type II isolators. In a Type I isolator, the pivot attached to the base is nearer to the isolator mass and in a Type II isolator, the pivot attached to the load is nearer to the isolator mass. Let us first analyze a base-excited Type I isolator, which is depicted in Fig. 3.

Let us assume that the lever rod is massless and rigid; the spring is linear, massless and undamped. Then, the system is sdof. Moreover, let us assume that the oscillations are small. Then, linear theory is applicable, generating the equation for z in terms of x and y as

$$z = \alpha y - (\alpha - 1)x, \quad \text{where } \alpha = l_1/l_2 > 1. \tag{20}$$

Moreover, the equation of motion is as follows:

$$(1 + \mu(\alpha - 1)^2)\ddot{x} + \omega_0^2 x = (\mu\alpha(\alpha - 1))\ddot{y} + \omega_0^2 y, \quad \text{where } \omega_0 = \sqrt{k/m}, \quad \mu = m_{\text{is}}/m. \tag{21}$$

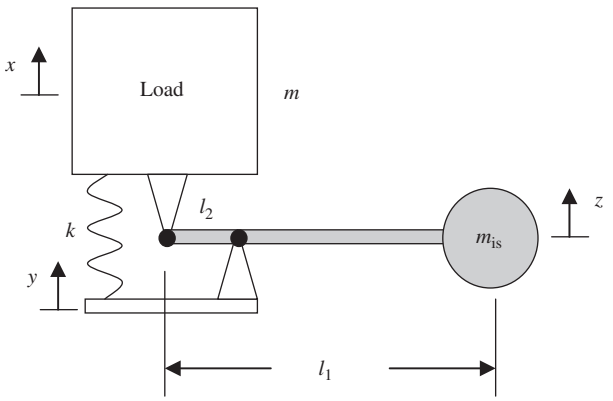

Fig. 3. Base-excited Type I isolator: here, y is the displacement of the base, x is the displacement of the load, z is the displacement of the isolator mass, k is the mount stiffness, m is the mass of the load, m_{is} is the isolator mass, l_1 is the length of the lever and l_2 is the distance between two pivot points.

It is important to notice that the effective mass of the system can be much larger than m, provided that the lever ratio α is large enough. Moreover, the inertial forcing term also increases with the lever ratio. Thus, with a small mass m_{is}, one can generate large inertia forces provided the lever ratio is large enough.

The right-hand side of Eq. (21) can be equal to zero when the excitation frequency is equal to

$$\omega_z = \frac{\omega_0}{\sqrt{\mu\alpha(\alpha-1)}} = \sqrt{\frac{k}{m_{\text{is}}\alpha(\alpha-1)}}. \tag{22}$$

We can see that ω_z is independent of m. Moreover, the pole of the system is at

$$\omega_p = \frac{\omega_0}{\sqrt{1+\mu(\alpha-1)^2}} = \sqrt{\frac{k}{m+m_{\text{is}}(\alpha-1)^2}}. \tag{23}$$

Then, $T(\omega)$ is obtained as

$$T(\omega) = \frac{(1-\omega^2/\omega_z^2)}{(1-\omega^2/\omega_p^2)}. \tag{24}$$

Moreover,

$$\frac{\omega_p}{\omega_z} = \sqrt{\frac{\mu\alpha(\alpha-1)}{1+\mu(\alpha-1)^2}}. \tag{25}$$

It can be seen that if $\mu = 1/(\alpha-1)$ then $\omega_p/\omega_z = 1$. Hence, pole and zero cancellation occurs, which imply that $T(\omega)$ is equal to one for all excitation frequencies. Furthermore, given α, if μ is greater than $1/(\alpha-1)$, then $\omega_p > \omega_z$ and if μ is less than $1/(\alpha-1)$, then $\omega_p < \omega_z$. Therefore, the order of the pole and the zero depends upon the values of α and μ.

Let us assume that $\omega_p/\omega_z \neq 1$ and calculate the bandwidth of the stop-band at a given value of T_0. As in the case of the DVA equipped system, let us try to solve for l and u.

$$\omega_0^2 = N^2\omega_z^2, \quad \omega_{s1}^2 = l^2\omega_z^2, \quad \omega_{s2}^2 = u^2\omega_z^2. \tag{26}$$

Eqs. (22) and (26) imply that

$$N = \sqrt{\mu\alpha(\alpha-1)} \Rightarrow \mu = N^2/(\alpha(\alpha-1)). \tag{27}$$

Eqs. (25) and (27) imply that

$$\frac{\omega_p}{\omega_z} = \sqrt{\frac{N^2\alpha}{(N^2+1)\alpha - N^2}}. \tag{28}$$

To determine u, let us substitute Eq. (28) in Eq. (24) and equate it to T_0. Then,

$$u = \frac{1}{\sqrt{1+(T_0/(1-T_0))\left(1/\alpha - 1/N^2\right)}}. \tag{29}$$

By definition, the lever ratio α is greater than one. Moreover, $N>1$ and $T_0 \ll 1$ imply that u can be approximated as

$$u \cong 1+\frac{T_0}{2(1-T_0)}\left(\frac{1}{N^2}-\frac{1}{\alpha}\right). \tag{30}$$

As before, l can be determined by replacing T_0 with $-T_0$ in Eq. (30).

$$l \cong 1-\frac{T_0}{2(1+T_0)}\left(\frac{1}{N^2}-\frac{1}{\alpha}\right). \tag{31}$$

In the bandwidth calculation of the DVA equipped system, u and l represented upper and lower stop-band frequency ratios. Hence, u was greater than l. However, in this system the order of u and l depends on the values of α and N. Therefore, the bandwidth calculation will involve an absolute value sign. Here is the approximate value of the bandwidth of a Type I anti-resonant vibration isolator:

$$BW_I = \left|\frac{u-l}{\sqrt{ul}}\right| \cong |u-l| \cong T_0\left|\frac{1}{N^2}-\frac{1}{\alpha}\right|. \tag{32}$$

If $\alpha>N^2$, then $\omega_p<\omega_z$ and the absolute value sign in Eq. (32) can be removed. Similarly, if $\alpha<N^2$, then $\omega_p>\omega_z$ and the absolute value sign in Eq. (32) can be removed provided that a minus sign is added in front of the equation.

To formulate bandwidth in terms of μ, let us solve for $\alpha>1$ in Eq. (27)

$$\alpha=\frac{1+\sqrt{1+\left(4N^2/\mu\right)}}{2}. \tag{33}$$

Then, $N>1$, $\mu>0$ and $T_0 \ll 1$ imply that

$$BW_I \cong T_0\left|\frac{1}{N^2}-\frac{2}{1+\sqrt{1+\left(4N^2/\mu\right)}}\right|. \tag{34}$$

If $\mu<1/(N^2-1)$, then $\omega_p<\omega_z$ and the absolute value sign in Eq. (34) can be removed. Similarly, if $\mu>1/(N^2-1)$, then $\omega_p>\omega_z$ and the absolute value sign in Eq. (34) can be removed provided that a minus sign is added in front of the equation.

If $\mu \ll 1$ then Eq. (34) can be simplified as

$$BW_I \cong T_0\left|\frac{1}{N^2}-\frac{\sqrt{\mu}}{N}\right|. \tag{35}$$

Here is an example with $N=2$ and $\mu=0.1$. Fig. 4 shows the transmissibility plots of the Type I isolator and the sdof mass–spring system without the isolator.

According to Eq. (34), bandwidth at $T_0=0.1$ can be calculated as 0.0104. This value is much larger than the bandwidth of the equivalent DVA equipped system, which was calculated as 0.0025.

Now, let us calculate bandwidth for a Type II anti-resonant vibration isolator, which is depicted in Fig. 5.

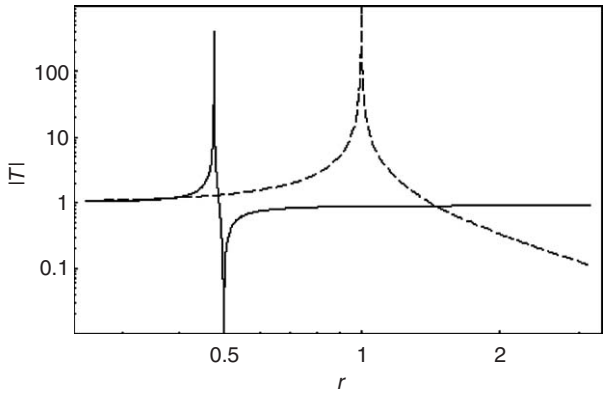

Fig. 4. Transmissibility plots showing the bandwidth of a Type I isolator for $N = 2$, $\mu = 0.1$:——, Type I isolator; – – – –, sdof mass–spring.

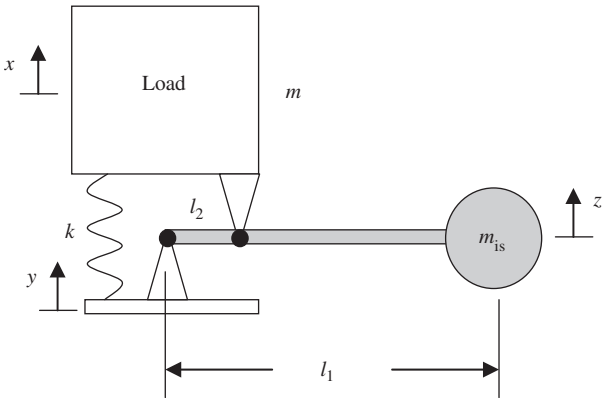

Fig. 5. Base-excited Type II isolator: here, y is the displacement of the base, x is the displacement of the load, z is the displacement of the isolator mass, k is the mount stiffness, m is the mass of the load, m_{is} is the isolator mass, l_1 is the length of the lever and l_2 is the distance between two pivot points.

Here is the equation of motion:

$$(1 + \mu\alpha^2)\ddot{x} + \omega_0^2 x = (\mu\alpha(\alpha - 1))\ddot{y} + \omega_0^2 y, \quad \text{where } \omega_0 = \sqrt{\frac{k}{m}}, \mu = \frac{m_{is}}{m}, \alpha = \frac{l_1}{l_2}. \tag{36}$$

In a Type II isolator, the effective mass of the system is larger. Hence, the pole of a Type II isolator is smaller than that of an equivalent Type I isolator.

$$\omega_p = \frac{\omega_0}{\sqrt{1 + \mu\alpha^2}} = \sqrt{\frac{k}{m + m_{is}\alpha^2}}, \tag{37}$$

ω_z is the same with an equivalent Type I isolator, which is given in Eq. (22). Moreover,

$$\frac{\omega_p}{\omega_z} = \sqrt{\frac{\mu\alpha(\alpha-1)}{1+\mu\alpha^2}} < 1 \quad \text{for} \quad \alpha > 1. \tag{38}$$

By definition, α is greater than one. Hence, in a Type II isolator ω_p is always less than ω_z. It can be seen that by replacing α with $(1-\alpha)$ in Eq. (36) one can obtain Eq. (21). Then, the bandwidth of a Type II isolator can be obtained by replacing α with $(1-\alpha)$ in Eq. (32)

$$BW_{II} \cong T_0 \left| \frac{1}{N^2} - \frac{1}{1-\alpha} \right| = T_0 \left| \frac{1}{N^2} + \frac{1}{\alpha-1} \right| = T_0 \left(\frac{1}{N^2} + \frac{1}{\alpha-1} \right). \tag{39}$$

Since ω_p is always less than ω_z, the absolute value sign is removed in the last step of Eq. (39). However, in order not to violate the approximation steps described by Eqs. (30)–(32), need $\alpha > 2$. This puts an upper bound on the value of μ due to Eq. (27), that is, $\mu < N^2/2$. Here is the formulation of bandwidth in terms of μ instead of α provided $N > 1$, $0 < \mu < N^2/2$ and $T_0 \ll 1$

$$BW_{II} \cong T_0 \left(\frac{1}{N^2} + \frac{2}{-1+\sqrt{1+\left(4N^2/\mu\right)}} \right). \tag{40}$$

If $\mu \ll 1$ then Eq. (40) can be further simplified as

$$BW_{II} \cong T_0 \left(\frac{1}{N^2} + \frac{\sqrt{\mu}}{N} \right). \tag{41}$$

Here is an example with $N = 2$ and $\mu = 0.1$. Fig. 6 shows the transmissibility plots of the Type II isolator and the sdof mass–spring system without the isolator.

According to Eq. (41), bandwidth at $T_0 = 0.1$ can be calculated as 0.0421. This value is much larger than the bandwidth of the equivalent Type I isolator, which was calculated as 0.0104 or the bandwidth of the equivalent DVA equipped system, which was calculated as 0.0025.

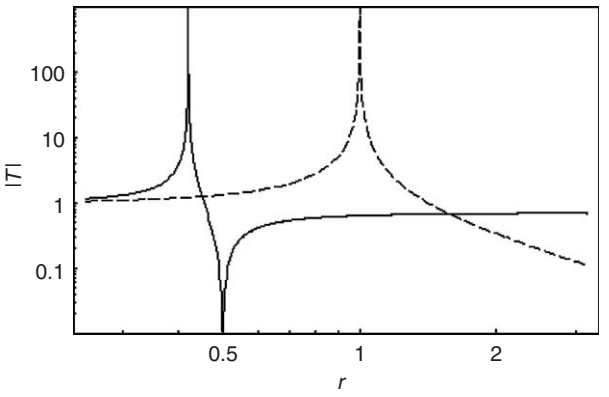

Fig. 6. Transmissibility plots showing the bandwidth of a Type II isolator for $N = 2$, $\mu = 0.1$:——, Type II isolator; – – – –, sdof mass–spring.

2.3. Bandwidth comparisons

The aim in this section is to compare bandwidth of DVA equipped systems, Type I and Type II isolators for $N>1$, $0<\mu<N^2/2$ and $T_0 \ll 1$.

Let us first compare Type I and Type II isolators according to Eqs. (32) and (39).

$$BW_I \cong T_0\left|\frac{1}{N^2}-\frac{1}{\alpha}\right|,\quad BW_{II} \cong T_0\left(\frac{1}{N^2}+\frac{1}{\alpha-1}\right).$$

First of all, both systems have the same dependence on T_0. According to Eq. (33), given μ and N, α is the same for both systems. By definition α is larger than one. Actually, if $\mu<N^2/2$, then according to Eq. (33) $\alpha>2$.

Suppose $\alpha \geqslant N^2$, then the absolute value sign in BW_I can be removed. Since N^2, α, $(\alpha-1)$ are all positive, BW_{II} is larger than BW_I. If $\alpha<N^2$, then the absolute value sign in BW_I can be removed by adding a minus sign in front of the equation. Since, $(\alpha-1)<\alpha$ and N^2 is positive, again BW_{II} is larger than BW_I. Therefore, BW_{II} is larger than BW_I for all $N>1$, $0<\mu<N^2/2$ and $T_0 \ll 1$.

Now, let us show that BW_{II} is larger than BW_a for all $N>1$, $0<\mu<N^2/2$ and $T_0 \ll 1$. In order to compare these two systems, their bandwidths should be given in terms of the same variables. Therefore, one may choose to compare Eqs. (19) and (40). However, it is easier to compare them by using the variable α. Actually, this variable is defined for lever-type anti-resonant vibration isolators and physically it is not relevant to DVAs. However, mathematically, given α and N, μ can be calculated using Eq. (27). Then,

$$\mu=\frac{N^2}{\alpha(\alpha-1)} \Rightarrow BW_a \cong T_0\frac{\mu}{N^2}=T_0\frac{1}{\alpha(\alpha-1)}. \tag{42}$$

Moreover,

$$\alpha>2 \Rightarrow \frac{1}{\alpha(\alpha-1)}<\frac{1}{\alpha-1} \Rightarrow \left(\frac{1}{N^2}+\frac{1}{\alpha-1}\right)>\frac{1}{\alpha(\alpha-1)} \Rightarrow BW_{II}>BW_a. \tag{43}$$

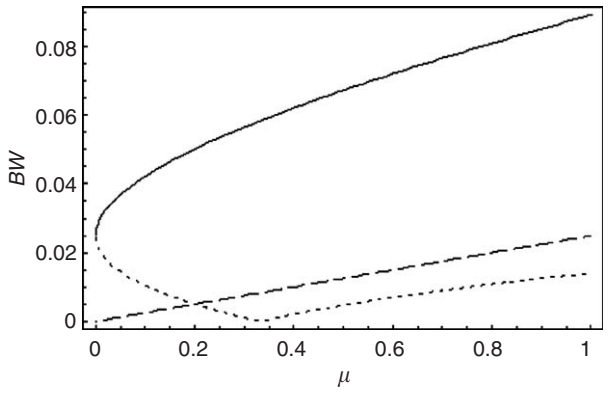

Fig. 7. Bandwidth versus μ comparisons for DVA equipped load (– – – –), Type I isolator (· · · · · ·) and Type II isolator (——) for $N=2$ and $T_0=0.1$.

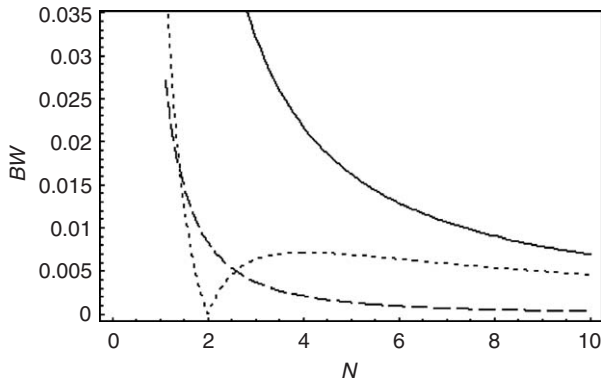

Fig. 8. Bandwidth versus N comparisons for DVA equipped load (– – – –), Type I isolator (· · · · · ·) and Type II isolator (——) for $\mu = \frac{1}{3}$ and $T_0 = 0.1$.

Thus, Type II isolator offers the largest bandwidth for any given $N > 1$, $0 < \mu < N^2/2$ and $T_0 \ll 1$. Let us now see the performance of these systems comparatively on graphs. To do that let us use Eqs. (19), (34) and (40).

$$BW_a \cong \frac{T_0\mu}{N^2}, \quad BW_I \cong T_0\left|\frac{1}{N^2} - \frac{2}{1+\sqrt{1+(4N^2/\mu)}}\right|, \quad BW_{II} \cong T_0\left(\frac{1}{N^2} + \frac{2}{-1+\sqrt{1+(4N^2/\mu)}}\right).$$

It can be seen that all the three systems have the same linear dependence on T_0. However, the dependence on μ and N are not straightforward.

Fig. 7 shows the dependence of bandwidth to μ, given $N = 2$ and $T_0 = 0.1$. Notice that $BW_I = 0$ when $\mu = 1/(N^2 - 1) = \frac{1}{3}$. Moreover, if $\mu < \frac{1}{3}$ then, $\omega_p < \omega_z$, and if $\mu > \frac{1}{3}$, then $\omega_p > \omega_z$. It can also be seen in Fig. 7 that as $\mu \to 0$, $BW_a \to 0$ and BW_I, $BW_{II} \to T_0/N^2 = 0.025$. However, Eq. (33) implies that, given N, if $\mu \to 0$, then $\alpha \to \infty$. Therefore, to reduce the isolator mass in low-frequency vibration isolation problems, one should be able to use a large lever ratio. This is the reason why hydraulic leverage is popular in the aerospace industry. Moreover, Fig. 8 shows the dependence of bandwidth to N, given $\mu = \frac{1}{3}$ and $T_0 = 0.1$.

So far, only systems with single anti-resonance frequencies were considered. In the next section a 2dof anti-resonant vibration isolator will be synthesized, analyzed and compared with the Type II isolator, which after all offers the largest bandwidth among the three systems.

3. Design of a wide-band vibration isolator

As mentioned before, both DVA equipped systems and anti-resonant vibration isolators have single anti-resonance frequency in their stop-bands. A natural way of increasing the bandwidth of a stop-band is to place additional anti-resonance frequencies. In this section, the aim is to synthesize an isolator that has two anti-resonance frequencies placed between two resonance frequencies. This design is the simplest wide-band vibration isolator.

3.1. Building blocks

Anti-resonant vibration isolators are the perfect building blocks for this design. First of all, it has been shown in Section 2.3 that Type II anti-resonant vibration isolator offers larger bandwidth than the other two systems for any given $N>1$, $0<\mu<N^2/2$ and $T_0 \ll 1$. Secondly, Type I anti-resonant vibration isolator offers control over the order of the pole and the zero by manipulating the values of α and μ. The order can be controlled because there is asymmetry in the inertial forcing terms generated by the levered mass. According to Eq. (21), the normalized values of the inertial forcing terms are $\mu(\alpha-1)^2$ and $\mu\alpha(\alpha-1)$. So, the former is always smaller than the latter for any $\alpha>1$ and as it was shown in Section 2.2, the pole-zero order depends whether μ or $1/(\alpha-1)$ is larger. If the inertial forces were equal, then the pole and the zero would be in the following form:

$$\omega_z=\frac{\omega_0}{\sqrt{f_i}},\quad \omega_p=\frac{\omega_0}{\sqrt{1+f_i}}\Rightarrow\frac{\omega_p}{\omega_z}=\sqrt{\frac{f_i}{1+f_i}}<1, \tag{44}$$

where f_i is the normalized value of the inertial forcing term. It can be seen in Eq. (44) that the pole would be always smaller than the zero. Hence, there would be no control over the order of the pole and the zero.

To obtain the desired pole-zero order in the 2dof system, one can choose a Type I isolator that has $\omega_{zI}<\omega_{pI}$ and a Type II isolator, which always has $\omega_{pI}<\omega_{zII}$ such that

$$\omega_{pII}<\omega_{zII}<\omega_{zI}<\omega_{pI}. \tag{45}$$

There are two different 2dof anti-resonant vibration isolator designs with these building blocks. In Design I, the lower stage is equipped with a Type I isolator and the upper stage is equipped

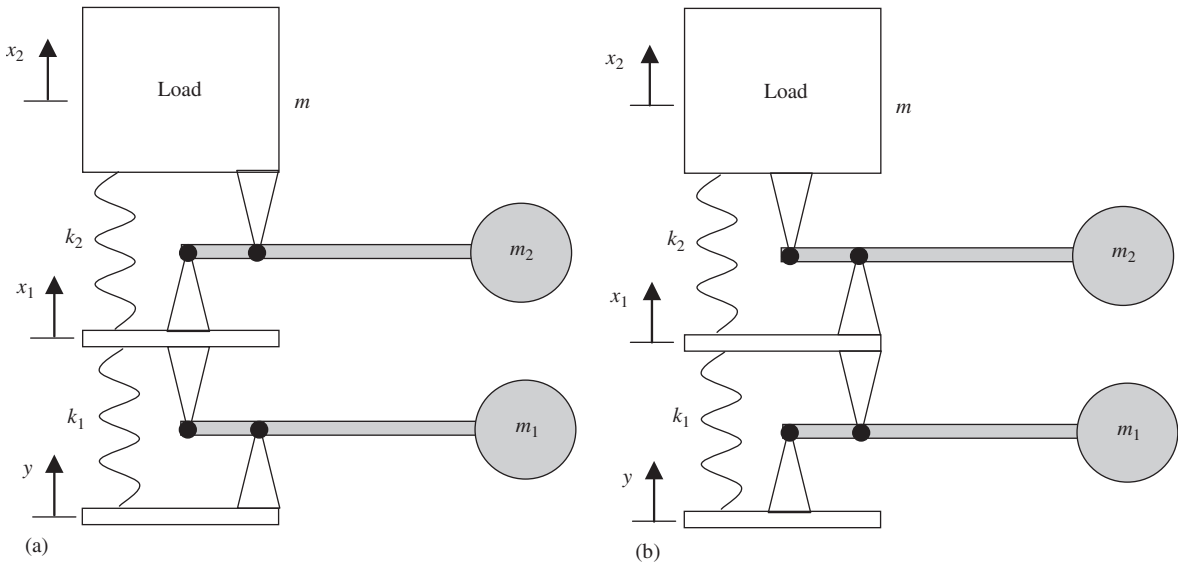

Fig. 9. (a) Design I and (b) Design II.

with a Type II isolator. In Design II, the lower stage is equipped with a Type II isolator and the upper stage is equipped with a Type I isolator. These two designs are shown in Fig. 9.

Let us first analyze Design I. Here are the equations of motion:

$$\mathbf{M}\ddot{\mathbf{X}} + \mathbf{K}\mathbf{X} = \mathbf{F}, \quad \text{where}$$

$$\mathbf{M} = \begin{bmatrix} m_1(\alpha_1 - 1)^2 + m_2(\alpha_2 - 1)^2 & -m_2\alpha_2(\alpha_2 - 1) \\ -m_2\alpha_2(\alpha_2 - 1) & m + m_2\alpha_2^2 \end{bmatrix}, \quad \mathbf{X} = \begin{bmatrix} x_1 \\ x_2 \end{bmatrix},$$
$$\mathbf{K} = \begin{bmatrix} k_1 + k_2 & -k_2 \\ -k_2 & k_2 \end{bmatrix}, \quad \mathbf{F} = \begin{bmatrix} k_1 y + m_1\alpha_1(\alpha_1 - 1)\ddot{y} \\ 0 \end{bmatrix}, \tag{46}$$

where y is the displacement of the base, x_i is the displacement of the ith stage, m_i is the mass of the ith isolator, m is the mass of the load, α_i is the lever ratio of the ith isolator stage, and k_i is the spring stiffness of the ith stage. It can be seen in Fig. 9(a) that the load is in the upper (2nd) stage and the plate combining the upper and lower (1st) stages is assumed to be massless.

First of all, let us identify the building blocks. In this design, k_1, m_1, α_1 are selected such that Type I isolator has $\omega_{zI} < \omega_{pI}$. Similarly, k_2, m_2, α_2 are selected such that Type II isolator has $\omega_{pII} < \omega_{zII}$. However, the effective loads in these two sub-systems are not equal. For the upper stage, the effective load is just m. But, for the lower stage, the effective load is $m + m_2$.

To see the Type II isolator independently, let $k_1 \to \infty$. Then, the lower stage behaves as if it is rigidly attached to the base. Hence, the system becomes a sdof system, which is composed of the upper stage only. Similarly, to see the Type I isolator independently, let $k_2 \to \infty$. Then, the upper stage behaves as if it is rigidly attached to the load. Hence, the system becomes a sdof system, which is composed of the lower stage only. Fig. 10 illustrates the two building blocks.

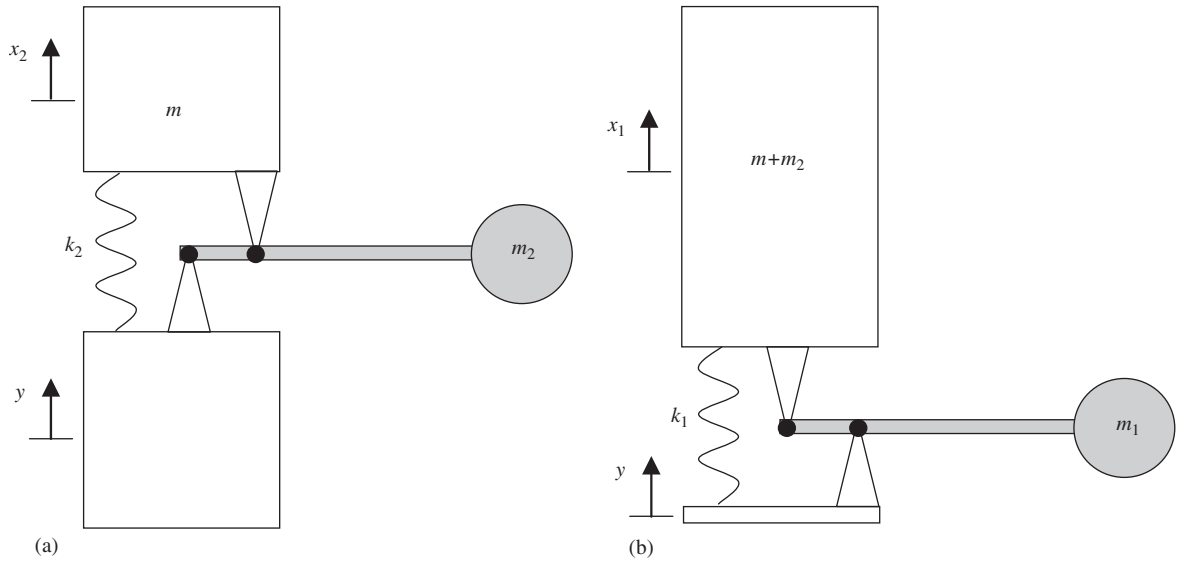

Fig. 10. (a) Type II isolator as one of the building blocks and (b) Type I isolator as the second building block.

The load is in the upper stage. Hence, to calculate the poles and zeros of the 2dof system represented by Eq. (46), transmissibility should be determined for the upper stage. Here is the transmissibility:

$$T(\omega) = \frac{\left(k_1 - \omega^2 m_1 \alpha_1(\alpha_1 - 1)\right)\left(k_2 - \omega^2 m_2 \alpha_2(\alpha_2 - 1)\right)}{(k_1 + k_2 - \omega^2 M_{11})(k_2 - \omega^2 M_{22}) - (k_2 - \omega^2 m_2 \alpha_2(\alpha_2 - 1))^2},$$
$$\text{where } M_{11} = m_1(\alpha_1 - 1)^2 + m_2(\alpha_2 - 1)^2, \quad M_{22} = m + m_2\alpha_2^2. \tag{47}$$

Now, let us compare the poles and zeros of this 2dof system with the two sdof building blocks. By comparing the numerator of Eq. (47) with Eq. (22), one can see that the zeros are of the same form with sdof isolators. Hence, the zero values do not change due to coupling of the two isolators. However, when these two sdof systems are combined into a 2dof system, the pole values change. This can be seen by equating the denominator of Eq. (47) to zero and solving for the poles and then comparing the result by Eqs. (23) and (37).

Let us name the poles and zeros of the 2dof system as ω_{p1}, ω_{p2}, ω_{z1}, ω_{z2}. It has been shown that the two zeros of the 2dof system is equal to the zeros of the building blocks. Let us label the zeros of the 2dof system as follows:

$$\omega_{z1} = \omega_{zI}, \quad \omega_{z2} = \omega_{zII}. \tag{48}$$

Moreover, let the smaller pole of the 2dof system be called as ω_{p2}. Now, let us compare ω_{p2} and ω_{pII}. ω_{pII} is the pole of the system represented by Fig. 10(a). ω_{p2} is the fundamental frequency of the 2dof system, which has a mode shape such that the both springs are either in tension or in compression. The added compliance from the lower stage decreases the force on the upper stage, which implies that $\omega_{p2} < \omega_{pII}$.

Secondly, let us compare ω_{p1} and ω_{pI}. ω_{pI} is the pole of the system represented by Fig. 10(b). ω_{p1} is the higher value pole of the 2dof system, which has a mode shape such that the springs are working antagonistically, that is, one is in tension while the other is in compression. This increases the force on the lower stage, which implies that $\omega_{p1} > \omega_{pI}$. Therefore, the order of the poles and zeros of the two building blocks and the 2dof system is as follows:

$$\omega_{p2} < \omega_{pII} < \omega_{zII} = \omega_{z2} < \omega_{zI} = \omega_{z1} < \omega_{pI} < \omega_{p1}. \tag{49}$$

One can deduce from Eq. (49) that the 2dof system has the desired order of the poles and zeros:

$$\omega_{p2} < \omega_{z2} < \omega_{z1} < \omega_{p1}. \tag{50}$$

Furthermore, coupling of the two building blocks, yielded a larger bandwidth compared to a system that has poles and zeros described by Eq. (45) since poles are further separated from the zeros.

After all, the aim is to obtain a system that obeys Eq. (50). To satisfy the initial assumption of $\omega_{zI} < \omega_{pI}$, m_1 should be larger than a certain value. However, in the combined system the pole value will increase, since $\omega_{p1} > \omega_{pI}$. Therefore, the initial assumption $\omega_{zI} < \omega_{pI}$ can be omitted provided Eq. (50) is still satisfied. This relaxation enables obtaining 2dof designs that satisfy Eq. (50) with smaller isolator masses.

Now, let us consider Design II. One can obtain the equations of motion for the second design by replacing α_i by $(1 - \alpha_i)$ in Eq. (46). It can be shown by a similar argument that this system also

satisfies Eqs. (49) and (50). However, in this design, Type II isolator is placed in the lower stage. The effective load on this stage is $m+m_2$, which is more than m. Hence, placing the Type II isolator in the lower stage instead of in the upper stage decreases its effective μ because of the extra load. According to Eq. (40), as μ decreases, the bandwidth of the Type II isolator decreases.

Similarly, placing the Type I isolator in the lower stage instead of in the upper stage decreases its effective μ. For a Type I isolator that has $\omega_{zI}<\omega_{pI}$, Eq. (34) can be rewritten as

$$BW_I \cong T_0\left(\frac{2}{1+\sqrt{1+\left(4N^2/\mu\right)}}-\frac{1}{N^2}\right) \text{ provided } N>1, \mu>\frac{1}{N^2-1} \text{ and } T_0 \ll 1. \tag{51}$$

Hence as μ decreases, the bandwidth of the Type I isolator also decreases. To compare the effect of decrease in μ to the decrease in bandwidth of Type I and Type II isolators, let us differentiate Eqs. (51) and (40) with respect to μ

$$\frac{\partial BW_I}{\partial \mu} \cong \frac{4N^2T_0}{\left(\mu^2\sqrt{1+\left(4N^2/\mu\right)}\right)\left(1+\sqrt{1+\left(4N^2/\mu\right)}\right)^2}, \tag{52}$$

$$\frac{\partial BW_{II}}{\partial \mu} \cong \frac{4N^2T_0}{\left(\mu^2\sqrt{1+\left(4N^2/\mu\right)}\right)\left(-1+\sqrt{1+\left(4N^2/\mu\right)}\right)^2}. \tag{53}$$

It can be seen that given $N>1$ such that $1/(N^2-1)<\mu<N^2/2$ and given $T_0 \ll 1$, Eq. (53) is larger than Eq. (52). Hence, bandwidth of Type II isolator is affected more due to a decrease in μ. This can also be seen by observing the slopes of the curves in Fig. 7 in Section 2.3 for the region where $\mu>1/(N^2-1)$. Thus, to obtain larger bandwidth in the 2dof system, Type II isolator should be placed in the upper stage. Therefore, Design I is preferred over Design II.

3.2. The optimization problem

In both sdof DVA equipped systems and sdof anti-resonant vibration isolators, given the mount stiffness k and the load mass m as parameters, there are two variables that should be determined in order to satisfy the requirements dictated by N, μ. The two variables are k_a and m_a for the case of a DVA equipped system and α and m_{is} for the case of sdof anti-resonant vibration isolators. μ determines the value of m_a or m_{is}, and N determines the value of k_a or α. Then, given T_0, there is a single value for the bandwidth. However, in Design I, there are more variables than the number of constraints. Therefore, there is the opportunity of maximizing bandwidth through optimization.

Before stating the optimization problem, let us make some definitions. Given $T(\omega)$ by Eq. (47) and given the maximum allowable transmissibility in the stop-band as T_0, ω_{s1} and ω_{s2} are the two solutions of $T(\omega)=-T_0$. Since there are two zeros in the stop-band, there is a frequency between the two zeros at which transmissibility attains a local maximum. Let us call this frequency as ω_{peak}. Moreover, all the frequencies are taken to be positive. Then, here is the statement of the

optimization problem

$$\begin{aligned}
&\text{maximize} && BW = \tfrac{\omega_{s2}-\omega_{s1}}{\sqrt{\omega_{s1}\omega_{s2}}}\\
&\text{subject to} && h_1 \;:\; T(\omega_{\text{peak}}) = T_0,\\
&&& h_2 \;:\; \tfrac{m_1+m_2}{m} = \mu,\\
&&& h_3 \;:\; \tfrac{k_1 k_2}{k_1+k_2} = k,\\
&&& h_4 \;:\; \sqrt{\omega_{s1}\omega_{s2}} = \omega_c = \omega_0/N, \;\text{ where } \omega_0 = \sqrt{k/m},\\
&&& k_1 \geq k,\;\; k_2 \geq k,\;\; m_1 \geq 0,\;\; m_2 \geq 0,\;\; \alpha_1 \geq 1,\;\; \alpha_2 \geq 1.
\end{aligned}$$

There are six variables in this problem, which are k_1, k_2, m_1, m_2, α_1 and α_2. As before, the mount stiffness k and the load mass m are the parameters that scale the band center frequency ω_c. To normalize the problem, k and m can be taken as one. Moreover, N, μ and T_0 are the parameters with the same definitions stated in Section 2.

There are six variables and four equality constraints. Let us call the variables k_2, m_2, α_1 and α_2 as state variables that satisfy the four equality constraints. The remaining two variables, k_1 and m_1, are called the decision variables.

The state variables m_2 and k_2 can easily be solved in terms of the decision variables using equality constraints h_2 and h_3, respectively. Although, ω_{s1}, ω_{s2}, ω_{peak} and $T(\omega_{\text{peak}})$ can be determined analytically, it is not feasible to solve for α_1 and α_2 analytically using the equality constraints h_1 and h_4. However, α_1 and α_2 can easily be determined via Newton's Method using the equality constraints h_1 and h_4. To determine the values of the decision variables that maximize bandwidth, any gradient-based algorithm can be used. In this paper, Newton's Method with variable step length is used in order not to violate the set constraints.

Given N, μ and T_0, to check whether the local maximum obtained through the optimization routine is actually a global maximum, different initial conditions are used. It has been observed that all the initial conditions gave the same output. Moreover, genetic algorithm is also used for various values of N, μ and T_0. Both methods converged to the same results. Therefore, it is highly probable that the search space has a single maximum for any reasonable value of N, μ and T_0.

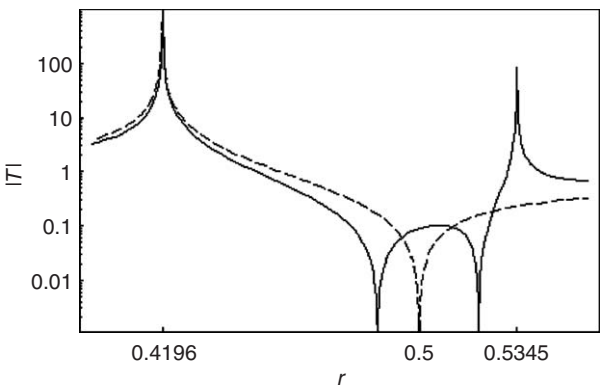

Fig. 11. Bandwidth comparison of a Type II isolator (– – – –) and the 2dof optimum design (——) for $N = 2$, $\mu = 0.1$ and $T_0 = 0.1$.

3.3. Numerical results

Let us compare the designs obtained through the optimization routine with the equivalent Type II isolators, which after all offer the largest bandwidth among the three isolation systems having single anti-resonance frequencies. In all the comparisons, let $k = 1$ and $m = 1$.

Let us first choose $N = 2$, $\mu = 0.1$ and $T_0 = 0.1$. For the Type II isolator $\mu = 0.1$, $m = 1 \Rightarrow m_{is} = 0.1$. Moreover, $\mu = 0.1$, $N = 2 \Rightarrow \alpha = 6.844$. For the 2dof optimum design, here are the values of the variables: $m_1 = 0.03384$, $m_2 = 0.06616$, $k_1 = 2.697$, $k_2 = 1.589$, $\alpha_1 = 17.65$, $\alpha_2 = 10.60$. Fig. 11 shows the transmissibility plots of the two systems.

By using Eq. (39) or (40) bandwidth of the Type II isolator can be found as 0.0421. Moreover, bandwidth of the optimum design is calculated as 0.0945. Let R_{bw} be the ratio of bandwidth of the optimum design to the bandwidth of the Type II isolator. Then, $R_{bw} = 2.24$. Hence, the optimum design has more than twice the bandwidth of the Type II isolator.

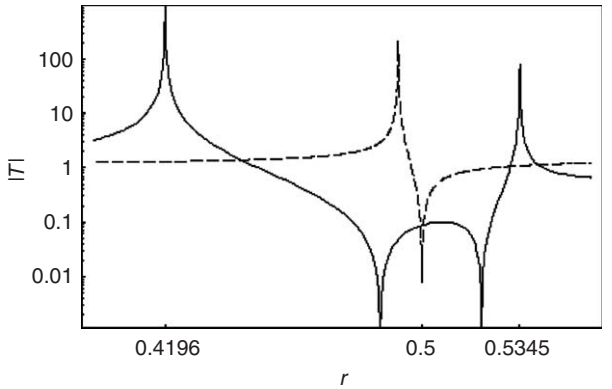

Fig. 12. Bandwidth comparison of a DVA equipped load (– – – –) and the 2dof optimum design (——) for $N = 2$, $\mu = 0.1$ and $T_0 = 0.1$.

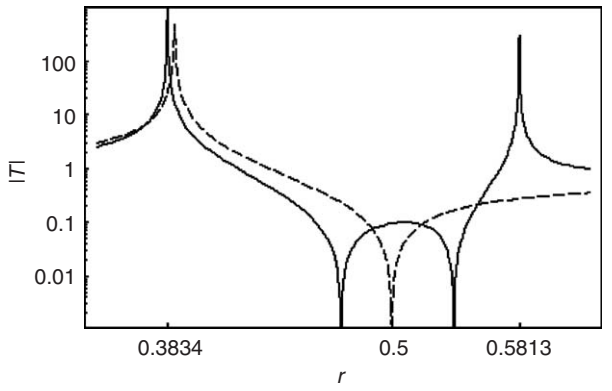

Fig. 13. Bandwidth comparison of a Type II isolator (– – – –) and the 2dof optimum design (——) for $N = 2$, $\mu = 0.5$ and $T_0 = 0.1$.

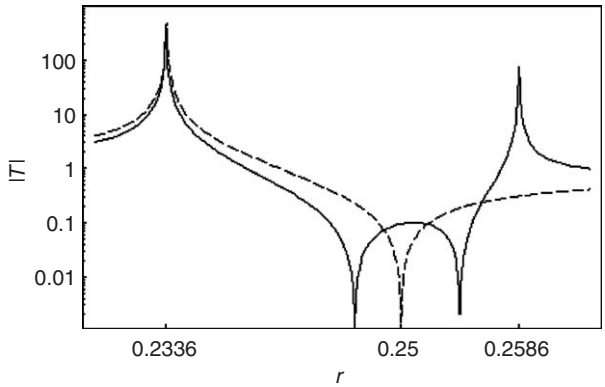

Fig. 14. Bandwidth comparison of a Type II isolator (– – – –) and the 2dof optimum design (——) for $N = 4$, $\mu = 0.1$ and $T_0 = 0.1$.

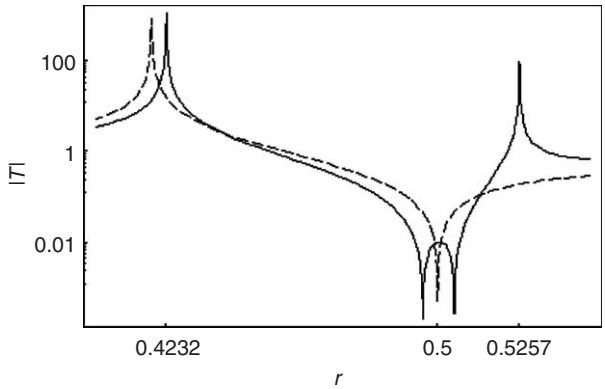

Fig. 15. Bandwidth comparison of a Type II isolator (– – – –) and the 2dof optimum design (——) for $N = 2$, $\mu = 0.1$ and $T_0 = 0.01$.

As shown earlier, a DVA equipped system would have much smaller bandwidth than an equivalent Type II isolator. Since DVA equipped systems are extensively used in industry, let us compare it with the optimum design in order to see the bandwidth improvement. Again let $N = 2$, $\mu = 0.1$ and $T_0 = 0.1$. Fig. 12 shows the transmissibility plots of the 2dof optimum design and an equivalent DVA equipped system.

As calculated earlier for the given parameters, the bandwidth of the optimum design is 0.0945, and the bandwidth of the DVA equipped system is 0.0025. So, the bandwidth ratio of these systems is almost 40, which is quite a large number.

In the following three comparisons, N, μ and T_0, will be changed one at a time. Hence, their individual effects will be seen. First, let us only change μ. Let, $N = 2$, $\mu = 0.5$ and $T_0 = 0.1$. Then, for the Type II isolator $m_{is} = 0.5$ and $\alpha = 3.372$. For the 2dof optimum design, here are the values of the variables: $m_1 = 0.09698$, $m_2 = 0.4030$, $k_1 = 1.752$, $k_2 = 2.329$, $\alpha_1 = 8.416$, $\alpha_2 = 5.631$. Fig. 13 shows the transmissibility plots of the two systems.

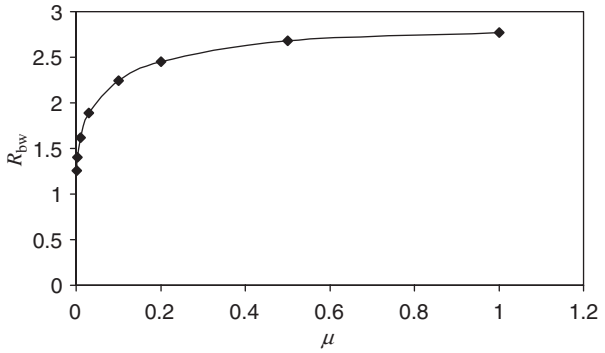

Fig. 16. Graph representing R_{bw} versus μ for $N = 2$ and $T_0 = 0.1$.

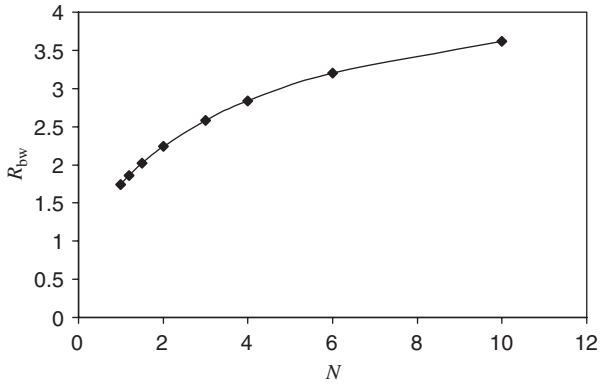

Fig. 17. Graph representing R_{bw} versus N for $\mu = 0.1$ and $T_0 = 0.1$.

Bandwidth of the Type II isolator is 0.0672. Moreover, bandwidth of the optimum design is 0.180. Therefore, $R_{bw} = 2.68$. So, in this case, the optimum design has almost three times the bandwidth of the Type II isolator.

Now, let us only change N. Let, $N = 4$, $\mu = 0.1$ and $T_0 = 0.1$. Then, for the Type II isolator $m_{is} = 0.1$ and $\alpha = 13.16$. For the 2dof optimum design, here are the values of the variables: $m_1 = 0.02349$, $m_2 = 0.07651$, $k_1 = 1.814$, $k_2 = 2.229$, $\alpha_1 = 35.06$, $\alpha_2 = 22.38$. Fig. 14 shows the transmissibility plots of the two systems.

Bandwidth of the Type II isolator is 0.0145. Moreover, bandwidth of the optimum design is 0.0411. Therefore, $R_{bw} = 2.84$. Thus, in this case, the optimum design has almost three times the bandwidth of the Type II isolator.

Finally, let us only change T_0. Let $N = 2$, $\mu = 0.1$ and $T_0 = 0.01$. Then, for the Type II isolator $m_{is} = 0.1$ and $\alpha = 6.844$. For the 2dof optimum design, here are the values of the variables: $m_1 = 0.01838$, $m_2 = 0.08162$, $k_1 = 1.575$, $k_2 = 2.740$, $\alpha_1 = 18.83$, $\alpha_2 = 12.20$. Fig. 15 shows the transmissibility plots of the two systems.

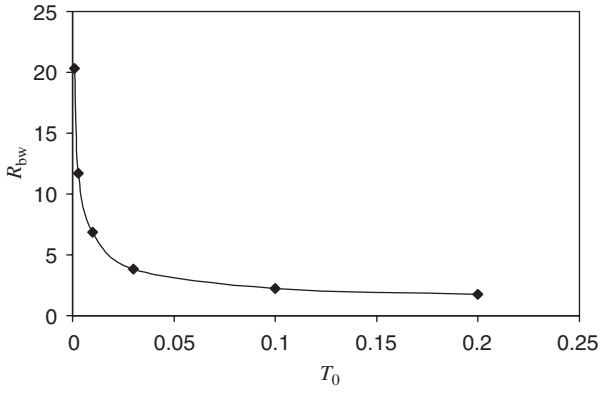

Fig. 18. Graph representing R_{bw} versus T_0 for $\mu = 0.1$ and $N = 2$.

Bandwidth of the Type II isolator is 0.00421. Moreover, bandwidth of the optimum design is 0.0272. Therefore, $R_{bw} = 6.84$. Hence, in this case, the optimum design has almost seven times the bandwidth of the Type II isolator.

The two systems can be compared for other values of N, μ and T_0. Figs. 16–18 show the effect of each parameter on R_{bw}. In each graph, only one parameter is changed at a time.

It can be inferred from these comparisons that R_{bw} increases as T_0 decreases or N increases. But, R_{bw} decreases as μ decreases. However, in all cases $R_{bw} > 1$. Hence, the 2dof design has larger bandwidth than the equivalent Type II isolator for the large range of parameters covered by Figs. 16–18.

It should be noted that all the isolation systems considered in this paper are undamped. In the presence of damping, bandwidth of all these systems would be smaller. So, in order to retain bandwidth, damping should be kept as small as possible. However, due to damping, wide anti-resonance notches would be affected less when compared to narrow notches. Therefore, bandwidth of Type II isolators and 2dof optimum designs would decrease less when compared to DVA equipped systems. A detailed analysis that includes damping can be the object of future research.

4. Conclusion

In this paper, bandwidths of sdof DVA equipped systems and lever-type anti-resonant vibration isolators are formulated using three non-dimensional numbers. The order of the pivot points plays an important role in the dynamics of lever-type anti-resonant vibration isolators. So, according to the order of their pivot points they are categorized as Type I and Type II anti-resonant vibration isolators. Based on the bandwidth formulations, which are derived for low-frequency applications, Type II anti-resonant vibration isolators offer the largest bandwidth among the three analyzed systems having single anti-resonance frequencies. Moreover, it has been shown that Type I anti-resonant vibration isolators offer control over the pole-zero order due to asymmetry in the inertial forcing terms generated by the levered masses. Then, a 2dof vibration

isolator is synthesized by stacking a Type I and a Type II isolator in series such that their stacking order yielded the maximum bandwidth in the optimization routine. Finally, the bandwidth improvement over the Type II isolator is demonstrated via parametric studies. To sum up, the 2dof system synthesized in this paper increased the applicability range of passive vibration isolation systems in the low-frequency range.

References

[1] L. Brillouin, *Wave Propagation in Periodic Structures: Electric Filters and Crystal Lattices*, McGraw-Hill, New York, 1946.
[2] O. Sigmund, J.S. Jensen, Systematic design of phononic band-gap materials and structures by topology optimization, *Philosophical Transactions of the Royal Society: Mathematical, Physical and Engineering Sciences* 361 (2003) 1001–1019.
[3] M.I. Hussein, Dynamics of Banded Materials and Structures: Analysis, Design and Computation in Multiple Scales, PhD Thesis, University of Michigan, 2004.
[4] H. Frahm, Device for damping vibrations of bodies, U.S. Patent No. 989,958, 1911.
[5] C.M. Harris, A.G. Piersol, *Harris' Shock and Vibration Handbook*, McGraw-Hill, New York, 2002.
[6] J.Q. Sun, M.R. Jolly, M.A. Norris, Passive, adaptive and active tuned vibration absorbers—a survey, *Transactions of American Society of Mechanical Engineers* 117 (1995) 234–242.
[7] W.G. Flannelly, Dynamic antiresonant vibration isolator, U.S. Patent No. 3,322,379, 1967.
[8] A.D. Rita, J.H. McGarvey, R. Jones, Helicopter rotor isolation evaluation utilizing the dynamic antiresonant vibration isolator, *Journal of the American Helicopter Society* 23 (1) (1978) 22–29.
[9] D. Braun, Development of antiresonance force isolators for helicopter vibration reduction, *Journal of the American Helicopter Society* 27 (4) (1982) 37–44.
[10] D. Braun, Vibration isolator particularly of the antiresonance force type, U.S. Patent No. 4,781,363, 1988.
[11] R.A. Desjardins, Vibration isolation system, U.S. Patent No. 4,140,028, 1979.
[12] R.A. Desjardins, W.E. Hooper, Antiresonant rotor isolation for vibration reduction, *Journal of the American Helicopter Society* 25 (3) (1980) 46–55.
[13] V.A. Ivovich, M.K. Savovich, Isolation of floor machines by lever-type inertial vibration corrector, *Proceedings of the Institution of Civil Engineers: Structures and Buildings* 146 (4) (2001) 391–402.
[14] E.I. Rivin, *Passive Vibration Isolation*, ASME Press, New York, 2003.
[15] A.J.H. Goodwin, Vibration isolators, U.S. Patent No. 3,202,388, 1965.
[16] D.R. Halwes, Vibration suppression system, U.S. Patent No. 4,236,607, 1980.
[17] M.R. Smith, W.S. Redinger, The model 427 pylon isolation system, *American Helicopter Society 55th Annual Forum*, Montreal, Canada, May 1999.
[18] D.P. McGuire, High stiffness (''rigid'') helicopter pylon vibration isolation systems, *American Helicopter Society 59th Annual Forum*, Phoenix, AZ, May 2003.
[19] P.E. Corcoran, G.E. Ticks, Hydraulic engine mount characteristics, SAE Paper # 840407, 1984.
[20] W.C. Flower, Understanding hydraulic mounts for improved vehicle noise, vibration and ride qualities, SAE Paper # 850975, 1985.
[21] M.R. Smith, R.J. Pascal, T. Lee, F.B. Stamps, M.C. van Schoor, B.P. Masters, C. Blaurock, E.F. Prechtl, J.P. Rodgers, D.J. Merkley, Results from the dynamically tailored airframe structures program, *American Helicopter Society 58th Annual Forum*, Montreal, Canada, June 2002.